An Approach for Improving Cirrus Cloud-Top Pressure/Height Estimation by Merging High-Spatial-Resolution Infrared-Window Imager Data with High-Spectral-Resolution Sounder Data

ELISABETH WEISZ, W. PAUL MENZEL, NADIA SMITH, RICHARD FREY, EVA E. BORBAS, AND BRYAN A. BAUM

Cooperative Institute for Meteorological Satellite Studies, University of Wisconsin—Madison, Madison, Wisconsin

(Manuscript received 8 August 2011, in final form 16 March 2012)

ABSTRACT

The next-generation Visible and Infrared Imaging Radiometer Suite (VIIRS) offers infrared (IR)-window measurements with a horizontal spatial resolution of at least 1 km, but it lacks IR spectral bands that are sensitive to absorption by carbon dioxide (CO_2) or water vapor (H_2O). The CO_2 and H_2O absorption bands have high sensitivity for the inference of cloud-top pressure (CTP), especially for semitransparent ice clouds. To account for the lack of vertical resolution, the ''merging gradient'' (MG) approach is introduced, wherein the high spatial resolution of an imager is combined with the high vertical resolution of a sounder for improved CTP retrievals. The Cross-Track Infrared Sounder (CrIS) is on the same payload as VIIRS. In this paper Moderate Resolution Imaging Spectroradiometer (MODIS) and Atmospheric Infrared Sounder (AIRS) data are used as proxies for VIIRS and CrIS, respectively, although the approach can be applied to any imager–sounder pair. The MG method establishes a regression relationship between gradients in both the sounder radiances convolved to imager bands and the sounder CTP retrievals. This relationship is then applied to the imager radiance measurements to obtain CTP retrievals at imager spatial resolution. Comparisons with *Cloud–Aerosol Lidar and Infrared Pathfinder Satellite Observation* (*CALIPSO*) cloud altitudes are presented for a variety of cloud scenes. Results demonstrate the ability of the MG algorithm to add spatial definition to the sounder retrievals with a higher accuracy and precision than those obtained solely from the imager.

1. Introduction

Upon launch of the Suomi National Polar-Orbiting Environmental Satellite Suite (NPOESS; since renamed the Joint Polar Satellite System, or JPSS) Preparatory Project (NPP) platform, the Visible and Infrared Imaging Radiometer Suite (VIIRS) will become the afternoon operational imager on the National Oceanic and Atmospheric Administration environmental polar-orbiting satellite platform and complement the Advanced Very High Resolution Radiometer (AVHRR) on the morning European polar-orbiting meteorological operations satellite (MetOp). In addition, a Fourier transform spectrometer called the Cross-Track Infrared Sounder (CrIS) will become the operational sounder on JPSS; the Infrared Atmospheric Sounding Interferometer (IASI) is the operational sounder on MetOp. The combinations of AVHRR with IASI and VIIRS with CrIS are intended to continue the measurements provided by the Moderate Resolution Imaging Spectroradiometer (MODIS) and the Atmospheric Infrared Sounder (AIRS) on the National Aeronautics and Space Administration (NASA) Earth Observing System (EOS). MODIS provides measurements at 36 different spectral bands at 1 km or better spatial resolution, including four bands in the 15-μm CO_2- and two in the 6.7-μm H_2O-sensitive spectral regions (King et al. 1992; Barnes et al. 1998). AIRS is a high-spectral-resolution infrared (IR) sounder with 2378 spectral bands between 3.7 and 15.4 μm and a nadir field of view (FOV) size of 13.5 km (Aumann et al. 2003; Chahine et al. 2006). IASI and CrIS will continue the record of high-spectral-resolution IR measurements that are important for cloud retrieval (cloud-top pressure and amount) and atmospheric sounding (vertical profiles of temperature, water vapor, and ozone and total column estimates of other trace gas species).

Corresponding author address: Elisabeth Weisz, Cooperative Institute for Meteorological Satellite Studies, University of Wisconsin—Madison, 1225 West Dayton St., Madison, WI 53706.
E-mail: elisabeth.weisz@ssec.wisc.edu

DOI: 10.1175/JAMC-D-11-0170.1

© 2012 American Meteorological Society

TABLE 1. Central wavelengths (CWL) for MODIS, VIIRS, and AVHRR IR-window spectral bands.

MODIS band	CWL (μm)	VIIRS band	CWL (μm)	AVHRR band	CWL (μm)
29	8.55	M14	8.55		
31	11.03	M15	10.80	4	10.80
32	12.02	M16	12.00	5	12.00

AVHRR and VIIRS are limited to window measurements in the IR spectrum; neither have any IR spectral bands located in water vapor (H_2O) or carbon dioxide (CO_2) absorption regions, and this will affect the inference of cloud-top properties (Heidinger et al. 2010). Table 1 lists the central wavelengths of the MODIS, VIIRS, and AVHRR IR-window spectral bands. Heidinger et al. (2010) discuss the consequences of that decision on the ability to estimate the cloud-top pressure for optically thin high cloud (cirrus); they found that the ability to infer cirrus cloud-top pressures/heights will be degraded over that from sensors that include even a single absorption band. Although VIIRS and AVHRR provide multiple IR-window measurements, the inclusion of even a single absorption band would greatly improve the vertical resolution of an optically thin ice cloud. Heidinger et al. (2010) show that for an example scene containing optically thin cirrus the spectral bands used by the operational VIIRS algorithm (Wong et al. 2007) have a vertical resolution of at least 200 hPa. With the inclusion of the single CO_2 band at 13.3 μm, however, the vertical resolution narrows to less than 30 hPa. The issue is not the algorithm but one of information content. The goal of this study is to demonstrate an approach to mitigate this issue for cloud-top pressure/height retrievals by merging data from both imager (e.g., AVHRR or VIIRS) and sounder (e.g., IASI or CrIS). This approach is applicable to morning orbit data from the *MetOp-A*/MetOp-B platform and the afternoon orbit data from Suomi NPP/JPSS.

In this paper, we use IWI to denote generic high-spatial-resolution IR-window imager measurements and HSRS to denote generic high-spectral-resolution sounder measurements. The combined imager-plus-sounder algorithm for cloud-top pressure determinations at imager resolution is demonstrated in this paper using IR-window measurements from MODIS for IWI and using the full spectral coverage from AIRS for HSRS. Past studies demonstrated the use of the hyperspectral IR bands for cloud-property retrieval (Zhou et al. 2007, 2009; Weisz et al. 2007b). Radiances observed by an imager and by a (collocated) sounder show consistency for most cloud fields (Kahn et al. 2007); this endorses the synergistic use of measurements from high-spatial-resolution imagers and high-spectral-resolution sounders. Synergistic use of imager and sounder measurements has been shown to improve cloud-top retrievals at sounder resolution (Li et al. 2004, 2005). An AIRS research algorithm that is based on eigenvector regression and was developed at the Cooperative Institute for Meteorological Satellite Studies/University of Wisconsin—Madison is used to derive AIRS-only sounding profiles (temperature, moisture, and ozone) and simultaneously cloud-top pressure (CTP) at single AIRS FOV resolution (Weisz et al. 2011; Smith et al. 2012). IWI-based cloud-top heights are derived using an optimal-estimation approach (Heidinger and Pavolonis 2009); this approach is applied to MODIS IR-window measurements. The CTP retrievals from combined imager (IWI) plus sounder (HSRS) are achieved using a "merging gradients" (MG) approach wherein a regression relationship is established between the HSRS CTP differences in neighboring FOVs and the associated IWI radiance differences.

Comparisons with EOS *Cloud Satellite* (*CloudSat*; Stephens et al. 2002; Marchand et al. 2008) and *Cloud–Aerosol Lidar and Infrared Pathfinder Satellite Observation* (*CALIPSO*; Winker et al. 2009) radar and lidar cloud-top height (CTH) measurements confirm the ability of both AIRS and MODIS to reveal valuable cloud information (Weisz et al. 2007c). *CALIPSO* products are used in this study to quantify the various cloud-height retrievals.

The MG-algorithm data requirements are summarized in section 2, with the method presented in section 3. *CALIPSO* CTHs are compared with those from IWI, HSRS, and IWI + HSRS for 10 different cloud scenes (each of them containing a variety of cloud types). The results for these case studies, with three cases presented in detail, are discussed in section 4. Section 5 concludes with further discussion and a summary of the results from this study.

2. Data

The MG method depends on three basic data types as input.

a. *Measured radiances from both IWI and HSRS instruments*

As mentioned in the introduction, the IR-window bands from MODIS (see Table 1) are used here to mimic an IWI instrument. MODIS operational measured radiances at 1-km resolution (products "MYD021KM" and "MYD03") are available online from the Level-1 and Atmospheric Archive and Distribution System (LAADS; http://ladsweb.nascom.nasa.gov/data/). The full IR spectrum (with bad channels excluded) of AIRS is used to

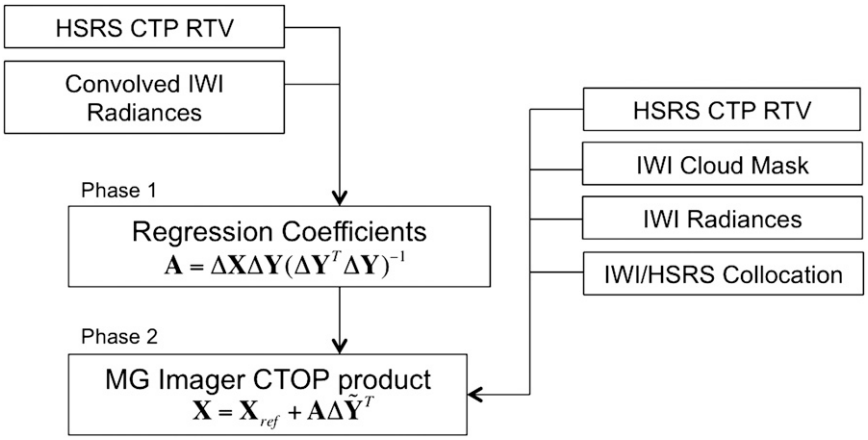

FIG. 1. Schematic outline of the main data inputs and mathematical steps of the MG CTP retrieval (RTV) algorithm. IWI and HSRS denote IR-window imager and high-spectral-resolution IR sounder, respectively.

mimic an HSRS instrument. The operational AIRS radiances (level-1B product) at ~14-km spatial resolution are available online from the Goddard Earth Sciences Data and Information Service Center (GES DISC; http://mirador.gsfc.nasa.gov/). Both AIRS and MODIS are on board the *Aqua* payload.

b. *The IWI cloud mask*

Again, the MODIS operational cloud mask (product "MYD35"; Strabala et al. 1994; Ackerman et al. 1998, 2008; Frey et al. 2008) was obtained from LAADS.

c. *A CTP/CTH for each single HSRS FOV*

With AIRS as the HSRS, the CTP retrievals are derived at single-FOV resolution from the dual-regression (DR) retrieval method (Weisz et al. 2011; Smith et al. 2012). The DR method, which uses statistical datasets stratified by cloud heights, provides accurate profile, surface, and cloud-property retrievals from high-spectral-radiance measurements under clear skies as well as below thin and/or scattered-to-broken cloud conditions.

3. Method

The dual imager–sounder approach employed in the MG algorithm is based on a set of assumptions: 1) HSRS measurements have more accurate information about cloud vertical structure than do IWI measurements, 2) IWI can provide subpixel definition to HSRS cloud properties, and 3) the correlation between IWI radiances and HSRS CTPs at low horizontal resolution is meaningful at high horizontal resolution.

A schematic diagram (Fig. 1) outlines the two main phases of the algorithm and how the data described in section 2 are employed at different stages in the method. Regression coefficients are calculated in phase 1, and CTP values are retrieved in phase 2. Both are described in more detail below.

a. *Regression-coefficient calculations*

In general, regression retrieval algorithms depend on a set of coefficients that define the relationship between top-of-atmosphere (TOA) radiance and the vertical atmospheric parameters (Weisz et al. 2007a; Smith et al. 2012). Such regression coefficients are calculated for data measured and retrieved from a single instrument. In the MG algorithm a relationship is defined between IWI measurements and HSRS CTP retrievals.

In the examples listed here, a set of dependent coefficients is calculated for each granule. This is done in two steps. First, the HSRS radiance measurements are convolved to the IWI spectral bands using the IWI spectral response functions. Tobin et al. (2006) examined the characterization of the MODIS spectral response functions by comparing MODIS radiance measurements with those from AIRS. The resulting HSRS radiance calculations have IWI spectral resolution but HSRS horizontal resolution. Second, for each cloudy FOV in an HSRS granule, regression coefficients $\mathbf{A}$ are calculated between the convolved IWI measurements and HSRS CTP retrievals as described in Eq. (1):

$$\mathbf{A} = \Delta\mathbf{X}\Delta\mathbf{Y}(\Delta\mathbf{Y}^{\mathrm{T}}\Delta\mathbf{Y})^{-1}, \tag{1}$$

where $\Delta\mathbf{X}$ refers to the HSRS CTP difference and is of dimension npar (number of retrieval parameters; here, npar = 1) × nsamps (number of samples) and $\Delta\mathbf{Y}$ is the matrix of convolved IWI radiance differences with

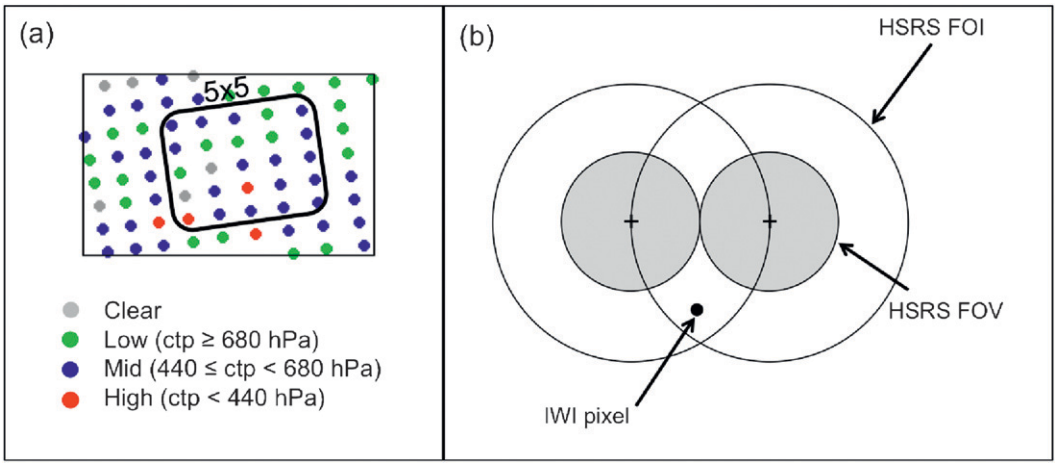

FIG. 2. (a) Schematic of an area of 5 × 5 HSRS FOVs containing clear and cloudy scenes. (b) Schematic of two overlapping HSRS FOIs surrounding the HSRS FOVs (shaded areas). One IWI pixel is shown as a black dot.

dimension nsamps × nbnds (number of spectral bands; here, nbnds = 3). Hence, at HSRS horizontal resolution, regression coefficients $\mathbf{A}$ are calculated with dimension npar × nbnds. Equation (1) follows a least squares logic and is derived from the relationship $\mathbf{\Delta X} = \mathbf{A\Delta Y}^{\mathrm{T}}$.

Because the relationship between TOA radiance and CTP is nonlinear, steps are taken to linearize the problem. For example, the coefficients are calculated from differences in CTPs for neighboring FOVs and the associated radiance differences. These differences are calculated as deviations from the mean of a regression training set (Weisz et al. 2007a; Smith et al. 2012). In the current context, however, differences are calculated as deviations from a neighborhood reference value. A neighborhood is defined as a 5 × 5 FOV area (Fig. 2a). The center FOV is set as the reference, and a difference $\mathbf{\Delta Y}$ is calculated for each of the remaining cloudy FOVs (maximum = 24). The rationale is to preserve as much of the data nuance at low horizontal resolution for high-horizontal-resolution application in the retrieval step.

To demonstrate the validity of this approach, a correlation coefficient is calculated between low-horizontal-resolution convolved IWI radiances and high-resolution IWI radiances for the 11-μm band (MODIS band 31) in a 5 × 5 HSRS FOV array. Correlation values between 0.3 and 0.9 have been calculated for the high clouds. This does validate assumption 3. The lower values occur in clouds of small horizontal extent, which are not resolvable by the sounder.

Another tactic for linearizing Eq. (1) is to calculate multiple sets of coefficients, each corresponding to a predefined cloud-height class. The International Satellite Cloud Climatology Project classification of low (>680 hPa), medium, and high (<440 hPa) cloud layers (Fig. 2a) has been adopted. Thus, three sets of coefficients corresponding to three different vertical layers are calculated.

b. MG retrieval

Once the low-horizontal-resolution regression coefficients are calculated, CTP is retrieved from high-horizontal-resolution IWI radiance measurements in two steps. First, IWI pixels are collocated to the HSRS FOV. A nearest-neighbor collocation strategy (Nagle and Holz 2009) is employed, but the collocation distance is enlarged to 2 times that of the HSRS FOV footprint radius, as depicted in Fig. 2b. This means that neighboring HSRS FOVs have overlapping clusters of associated IWI measurements. This overlapping area is referred to as the field of influence (FOI). The reason for this enlarged FOI is to maintain spatial consistency with the coefficients derived in section 3a and also to act as a smoothing function for CTP retrievals from adjacent FOIs.

In the second step, CTP is linearly regressed from cloudy IWI radiance measurements, or rather, from cloudy IWI radiance differences. Unlike the differences calculated for the coefficient calculation, the IWI radiance differences are calculated for each cloudy IWI pixel as the deviation from the mean of all (clear and cloudy) IWI pixels in the HSRS FOI. A CTP is retrieved for each IWI pixel by applying the regression coefficients $\mathbf{A}$ to a cloudy IWI radiance difference, denoted by $\mathbf{\Delta\tilde{Y}}$, as follows:

$$\mathbf{X} = \mathbf{X}_{\mathrm{ref}} + \mathbf{A\Delta\tilde{Y}}^{\mathrm{T}}, \tag{2}$$

where $\mathbf{X}_{\mathrm{ref}}$ denotes the HSRS CTP value of the FOI.

Note that IWI measurements are identified as cloudy on the basis of the IWI cloud mask product. The height class of the FOI HSRS CTP value determines the

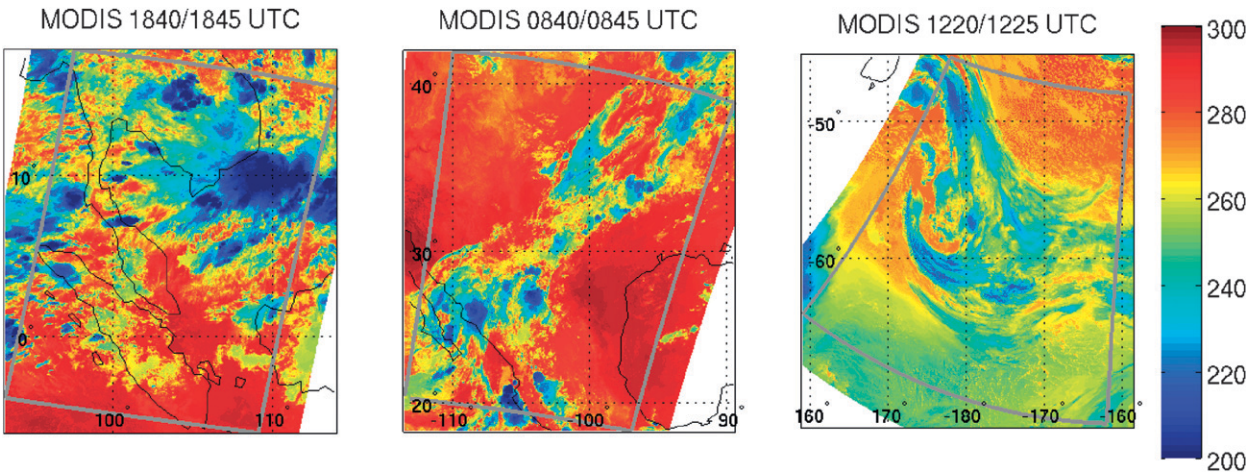

FIG. 3. MODIS 11-μm band-31 brightness temperature data (K) collocated with AIRS granules 187, 87, and 124 (indicated by the gray outlines) for 28 Aug 2006.

coefficient set (i.e., low, medium, or high) to apply for all of the associated IWI radiances in the FOI. In other words, if the HSRS CTP is classified as ''low,'' then low-cloud coefficients will be applied to all cloudy IWI pixels in the FOI.

As a result of the overlap between adjacent FOIs, some IWI measurements fall into more than one HSRS FOV (there can be a maximum of four). This means that for these cases there may be more than one CTP retrieval for an IWI pixel. At this time, a solution is found by averaging these CTP retrievals to achieve a CTP gradient between adjacent FOIs. This solution of averaging works well when two adjacent HSRS FOVs fall into the same height class, but it becomes more problematic otherwise. For this case (i.e., when high- and low-cloud retrievals for the same pixel are available), alternatives to averaging need to be investigated (e.g., such a retrieval can be flagged as low quality). This will be explored in future research. Other future research questions include finding an optimal regression distance for HSRS coefficient neighborhoods. Currently, a 5×5 neighborhood yields a robust statistical sample size for the coefficient calculation, but a 3×3 neighborhood may strengthen the relationship between radiance and CTP at the already coarse HSRS horizontal resolution. For the FOI, the radius could be enlarged or an inverse-distance weighting could be applied to the IWI pixels during retrieval. In addition, independent coefficient sets could prove more effective than the current dependent set that is calculated for each granule individually, especially since they can be calculated once and applied to any number of granules afterward. It may also be meaningful to classify coefficient calculation according to latitudinal regions (e.g., tropical, midlatitude, and high latitude).

4. Results

Retrieval results and comparisons are presented for a number of different granules for 28 August 2008. As described in section 2, AIRS is used as a proxy for HSRS to derive an HSRS-alone CTP product at single-FOV (~14 km) resolution; MODIS IR-window measurements are used for IWI data to derive the IWI + HSRS CTP product from the MG algorithm at 1-km spatial resolution. MODIS IR-window measurements were also used to derive an IWI-alone product at 5-km resolution from an optimal-estimation algorithm (Heidinger and Pavolonis 2009; Heidinger et al. 2010). The CTPs from these are converted to CTHs and are compared with the 5-km CTH product from the Cloud–Aerosol Lidar with Orthogonal Polarization (CALIOP) on board *CALIPSO* (Winker et al. 2009).

Several different cloud scenes have been investigated; three are presented in detail and are shown in Fig. 3 in terms of MODIS band-31 (11 μm) brightness temperatures. The *CloudSat* level-2 Cloud Profiling Radar cloud-classification (2B-CLDCLASS) product (Mace et al. 2007; Wang and Sassen 2001) was used to identify HSRS granules that represent a variety of cloud scenes. In addition, information on optically thin high clouds was obtained from CALIOP. Hence, these case studies include a variety of cloud types and geophysical conditions. The first case (AIRS granule 187) describes a deep convective system in the tropics, the second case (AIRS granule 087) contains scattered altostratus located in the

TABLE 2. Cloud-height statistics and description of cloud scenes for CALIOP minus IWI, HSRS, and IWI + HSRS (I+H) for 10 AIRS granules for 28 Aug 2006. The first three granules are explored in detail in section 4. Here, DC indicates deep convection.

		Bias (km)			Std dev (km)			
Granule	No. of samples	IWI	HSRS	I+H	IWI	HSRS	I+H	Description
187	1238	4.13	1.97	2.01	2.90	2.70	2.53	Tropical widespread DC and cirrus
87	845	3.19	0.69	0.75	3.49	2.36	1.96	Midlatitude scattered altostratus and cirrus
124	756	4.33	1.82	1.88	3.10	2.87	2.76	Polar nimbo- and altostratus with cirrus
47	912	3.76	1.00	1.32	4.75	4.38	3.69	Tropical scattered cirrus and low-level clouds
70	1007	2.44	1.13	1.24	3.76	3.60	3.34	Midlatitude altostratus and stratocumulus
71	531	4.82	1.63	1.98	5.62	4.42	3.84	Tropical DC and cirrus of small horizontal extent
86	838	1.27	0.57	0.59	1.62	2.01	1.76	Low-latitude thick nimbo- and altostratus
180	750	3.19	−0.20	−0.08	4.06	2.90	2.34	Tropical cyclone with DC and cirrus
197	799	1.15	0.43	0.50	3.54	2.84	2.37	Midlatitude narrow DC towers and cirrus
213	538	4.69	2.20	2.36	5.01	4.09	3.76	Tropical DC and broken cirrus
Total	8214	3.22	1.12	1.24	3.64	3.14	2.77	

midlatitudes (Northern Hemisphere), and the third case (AIRS granule 124) presents a polar system with nimbo- and altostratus. All three case studies contain thin cirrus as well.

The CTH statistics of CALIOP minus IWI/HSRS/IWI + HSRS differences are given in Table 2; the values were calculated for all CALIOP pixels at 5-km spatial resolution within the 10 AIRS granules (with the 3 granules mentioned above listed at the top of the table), as well as for the total of those granules. To obtain the same number of samples for all three differences (i.e., CALIOP minus IWI, CALIOP minus HSRS, and CALIOP minus IWI + HSRS), one HSRS FOV (~14 km) corresponds to multiple CALIOP pixels and IWI + HSRS values at 1-km spatial resolution that belong to the same CALIOP pixel are averaged. Figure 4 illustrates the collocation of the IWI, IWI + HSRS, and CALIOP within one HSRS FOV. In this example, the resolution of the IWI product is 5 km, although other imagers have higher spatial resolution (e.g., 1 km). In practice, the collocation among the different instruments is based on the technique described in Nagle and Holz (2009).

The total bias and standard deviation are computed as the sum of the individual values, weighted by the respective number of samples, and divided by the total number of samples. Only CTHs above 2 km were considered, since our focus is on improving the inference of optically thin high clouds at the higher spatial resolution of the imager. With respect to CALIOP, the total biases (standard deviations) for IWI, HSRS, and IWI + HSRS are 3.2, 1.1, and 1.2 km (3.6, 3.1, and 2.8 km) respectively. For the standard deviations, the IWI + HSRS shows the best overall comparison with CALIOP; and the bias for IWI + HSRS is comparable to that of HSRS alone but is considerably smaller than the bias for IWI alone.

When investigating these statistical values, differences in instrument characteristics (e.g., spatial and spectral resolution or spectral sensitivity to the retrieval parameter), retrieval methods, and measurement times have to be taken into consideration. In general, a lidar finds higher cloud tops because it is very sensitive to the presence of small particles. IR-derived retrievals tend to assign CTHs within the cirrus where the optical thickness is roughly 1 (Holz et al. 2008) and thus are below the CALIOP cloud heights. The three cases shown in Fig. 3 are discussed in greater detail below.

a. *Case 1: Tropical deep convective clouds and associated cirrus (AIRS granule 187; 28 August 2006)*

Tropical deep convective clouds often occur with transparent cirrus over the cloud towers. In this situation, for which the cloud is of vertical extent less than 1 km, the HSRS capability to resolve fine vertical structure is essential to find the proper cloud height. Retrievals from HSRS, IWI, and IWI + HSRS for AIRS granule 187 (28 August 2006) over Southeast Asia are shown in Fig. 5 for the entire granule (top row) and for a selected area

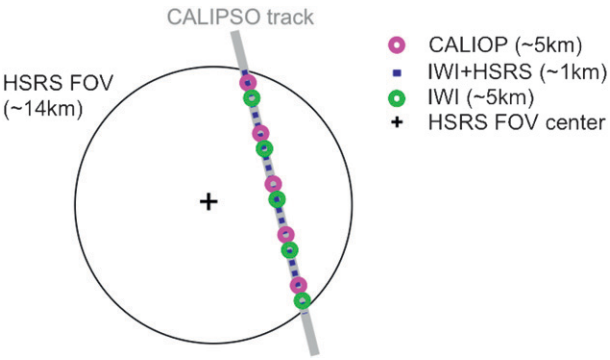

FIG. 4. Schematic diagram of the collocation of the IWI (green circles), IWI + HSRS (blue squares), and CALIOP (pink circles) within one HSRS FOV.

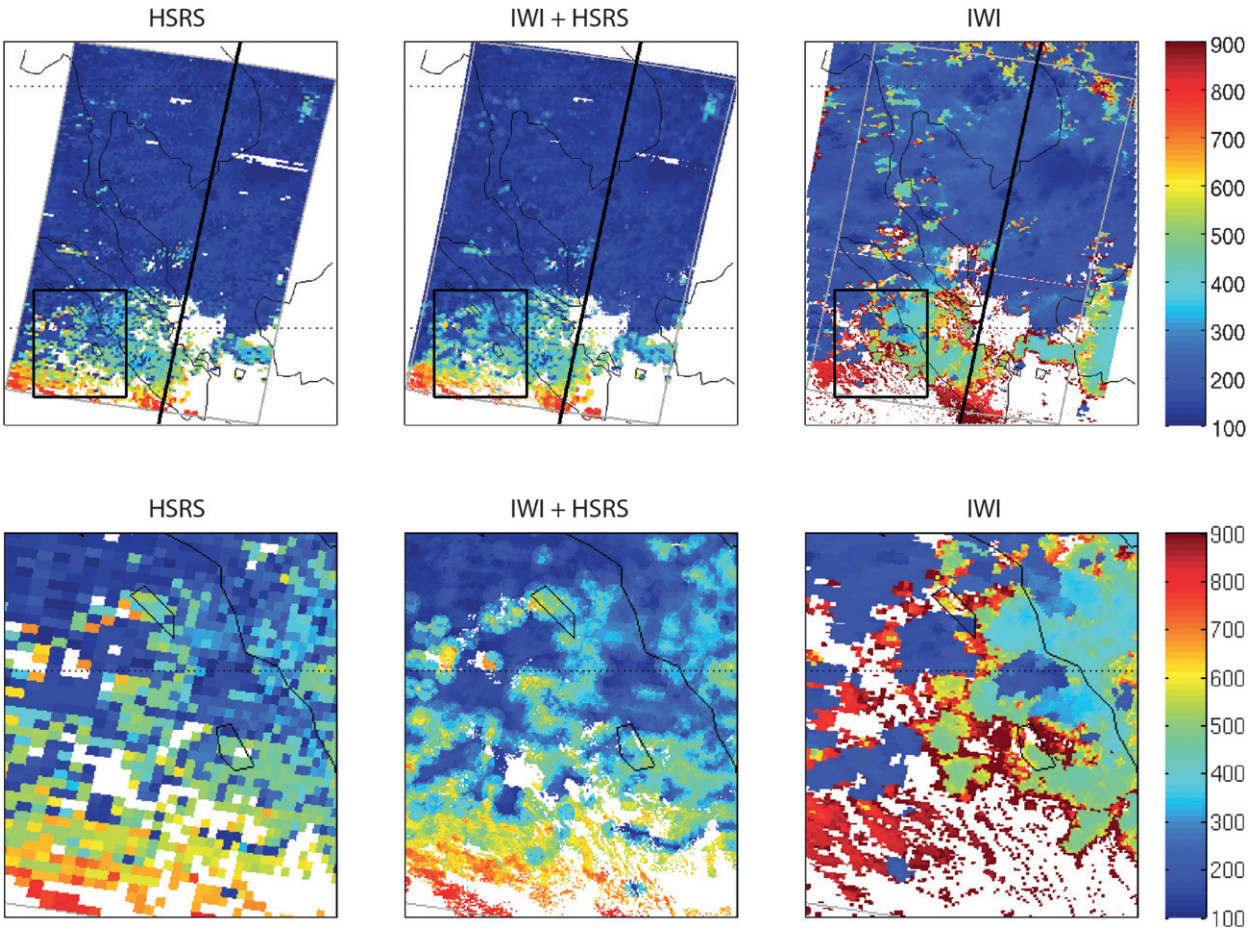

FIG. 5. CTP retrievals (hPa) from (left) HSRS, (center) IWI + HSRS, and (right) IWI for AIRS granule 187 (28 Aug 2006). (top) Entire granule (indicated by the gray outlines), with the *CALIPSO* overpass (black line) and the outlines of a selected area (black rectangle) shown. (bottom) As in the top row, but for the selected area shown in the black rectangles from the top row.

(bottom row). Recall that the nadir spatial resolution is ~13.5 km for HSRS retrievals, 5 km for IWI, and 1 km for IWI + HSRS retrievals. White areas indicate clear skies in the IWI CTP images, and in the HSRS and IWI + HSRS CTP images they may occasionally indicate unsuccessful CTP retrievals as a result of bad radiances. The IWI + HSRS CTP image shows some of the finer details missing in the HSRS CTP image.

This case contains a large area of deep convection. The extent of the cirrus fanning out from the center of the system at 13° latitude is found to be very similar by all three retrieval approaches (HSRS, IWI, and IWI + HSRS). Figure 6 shows the cloud-height retrievals (km) superimposed on the CALIOP 532-nm total attenuated backscatter (the lighter the color is, the stronger is the backscatter).

The deep convective cloud system is present from latitudes 8° to 15° with overlying thin cirrus starting around latitude 3°. HSRS captures the height of deep convection as well as the thin cirrus layer above. IWI is giving heights that are indicative of unit optical thickness within the cloud. HSRS-detected cloud heights agree extremely well with the CALIOP products (e.g., at latitudes from 2° to 4°, around 9°, and around 14°); the combined IWI + HSRS retrievals on occasion outperform the HSRS results, whereas IWI is not able to detect the thin cirrus layer. Table 2 shows that biases (standard deviations) for IWI, HSRS, and IWI + HSRS are 4.1, 2.0, and 2.0 km (2.9, 2.7, and 2.5 km), respectively.

One limitation of HSRS cloud retrievals is in detecting spurious cirrus of small horizontal extent (Kahn et al. 2008). For example, HSRS has difficulty in finding the cirrus around −4° and −1°.

b. Case 2: Midlatitude scattered altostratus and thin cirrus (AIRS granule 87; 28 August 2006)

This granule is located mostly over land (southern United States and Mexico). The CTP retrievals of HSRS, IWI, and IWI + HSRS in Fig. 7 show similar

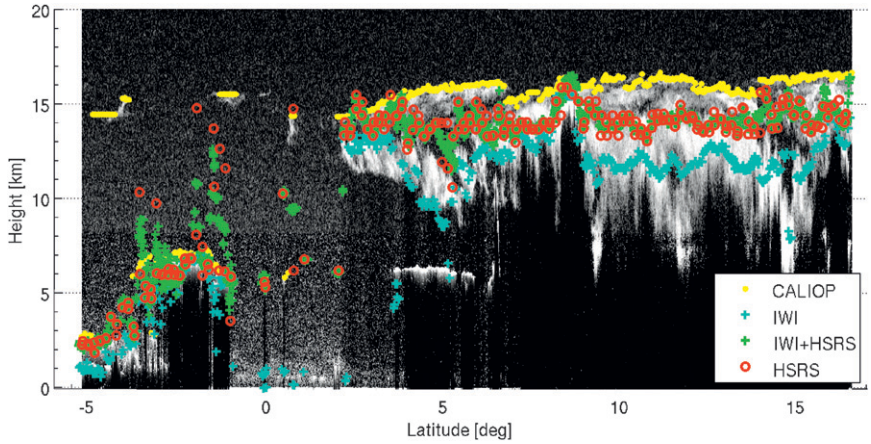

FIG. 6. Cross section along the *CALIPSO* track for AIRS granule 187 (28 Aug 2006). Shown in the background is CALIOP 532-nm total attenuated backscatter per kilometer per steradian. CTHs from CALIOP, IWI, IWI + HSRS, and HSRS are plotted as yellow dots, cyan plus signs, green plus signs, and red circles, respectively.

features of mid- and high-level clouds (cirrus, altostratus, and altocumulus). As seen in the zoomed-in area in the bottom row of Fig. 7, IWI detects large uniform areas of slightly higher CTPs whereas the IWI + HSRS shows more small-scale variations in CTP. Table 2 shows that biases (standard deviations) for IWI, HSRS, and IWI + HSRS are 3.2, 0.7, and 0.8 km (3.5, 2.4, and 2.0 km), respectively.

The comparisons with CALIOP retrievals are shown in Fig. 8. In the region between latitudes 20° and 22°, IWI underestimates the actual cirrus CTHs given by CALIOP, but the IWI + HSRS results are able to approach CALIOP values of this cirrus cloud. The deep convective element at latitude 31° is very well depicted by all three retrieval methods. The small transparent cloud around latitude 26° is captured by the HSRS and IWI + HSRS retrievals but not by the IWI retrievals. Most of the thin cirrus clouds with CTHs higher than 12 km between latitudes 29° and 39° are captured by IWI + HSRS but not by IWI.

c. *Case 3: Polar nimbo- and altostratus with cirrus overlay (AIRS granule 124; 28 August 2006)*

Granule 124 is located in the Southern Hemisphere (southeast of New Zealand) entirely over ocean. The HSRS, IWI, and IWI + HSRS retrievals in Fig. 9 agree on the extent and distribution of the cloud field, but the IWI retrievals find higher CTP values (i.e., lower cloud heights) in general.

Comparison with the CALIOP cloud-altitude product is shown in Fig. 10. For the cloud features (nimbo- and altostratus) between latitudes −65° and −54°, the heights of the cirrus clouds (as given by CALIOP) agree with the cloud heights retrieved from HSRS and IWI + HSRS; IWI heights are lower by 4–5 km, placing the CTHs within the cloud observed by CALIOP. Biases (standard deviations) for IWI, HSRS, and IWI + HSRS are 4.3, 1.8, and 1.9 km (3.1, 2.9, and 2.8 km), respectively (Table 2).

North of latitude −53°, a row of stratocumulus clouds resides very close to the ground (also evident in Fig. 3). The IWI values underestimate the CALIOP CTHs, whereas HSRS and IWI + HSRS heights are somewhat too high and show excessive vertical variation; this is likely caused by the HSRS difficulty in capturing these scattered cloud fragments that have little thermal contrast with clear skies. For latitudes from −54° to −52°, a two-layer cloud structure is observed; because our current HSRS retrieval algorithm does not account for two-layer situations, the retrieved product from HSRS and IWI + HSRS does not capture the lower clouds.

5. Summary and discussion

This paper reports on an approach to combine the horizontal detail of an IR-window imager instrument (using MODIS data as proxy) with the vertical resolution of a high-spectral-resolution infrared sounder instrument (using AIRS data as proxy) for cloud detection and cloud-top pressure estimation. At HSRS horizontal resolution (about 13.5 km at nadir), cloud structures are related to IWI radiance measurements through a regression relationship of HSRS CTP gradients against IWI measurements convolved to IWI spectral-band response functions. The resulting regression relationship is then applied to IWI radiance measurements at IWI horizontal resolution to determine CTPs at subkilometer

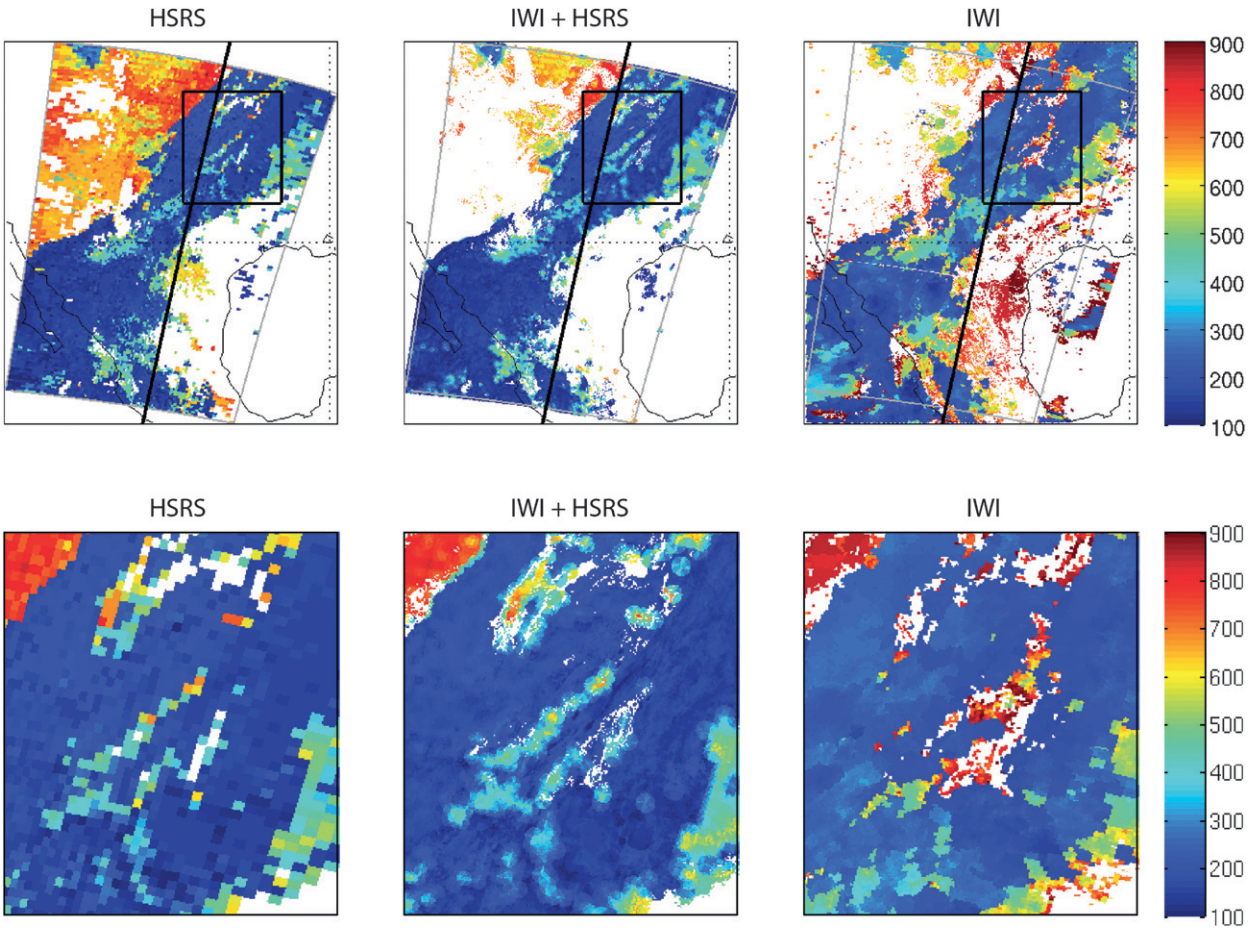

FIG. 7. As in Fig. 5, but for AIRS granule 87.

resolution. That is, the IWI + HSRS merging-gradients approach provides cloud pressures/heights at 1-km spatial resolution.

The MG CTPs are converted to CTH and are compared with the CALIOP, version 3, cloud product. For optically thin ice clouds and also for clouds of small vertical extent, the combined IWI + HSRS CTHs compare much better to CALIOP than do the individual IWI CTHs. The retrieval performance is found to be best for high clouds above 6 km. Difficulties arise for low and broken clouds of small horizontal extent that are not resolved by the sounder. IWI + HSRS biases for all of the cloud scenes with respect to CALIOP are 1.2 km, down from 3.2 km for IWI alone and corresponding to a bias reduction of 2.0 km. Note also that these bias values are comparable to those from the HSRS alone (1.1 km), but with an improved standard deviation of 2.8 km as compared with 3.1 km (from HSRS alone) and 3.6 km (from IWI alone). With this result, our expectation for the MG algorithm is met; in other words, this result demonstrates that it is possible to preserve the vertical resolution of HSRS measurements at a high spatial resolution.

We conclude that the dual-instrument MG algorithm presented in this paper yields CTP values that are at least as good as those retrieved from HSRS radiances alone but with an order-of-magnitude improvement in the spatial resolution. The objective of the MG (or IWI + HSRS) algorithm is to combine vertical information from the HSRS with spatial information from the IWI to produce a CTP retrieval product at IWI horizontal resolution but with HSRS vertical information. Because of a lack of vertical information in the IWI radiances, the IWI + HSRS CTP product accuracy cannot exceed that of the HSRS product alone. In a similar way, because of the lack of horizontal resolution in the HSRS radiances, the IWI + HSRS retrieved cloud field cannot improve on that retrieved from the IWI radiances alone. With the combined IWI + HSRS algorithm, however, it is possible to define CTP with higher accuracy at IWI horizontal resolution than is possible with IWI radiances alone; the latter typically underestimates cirrus clouds.

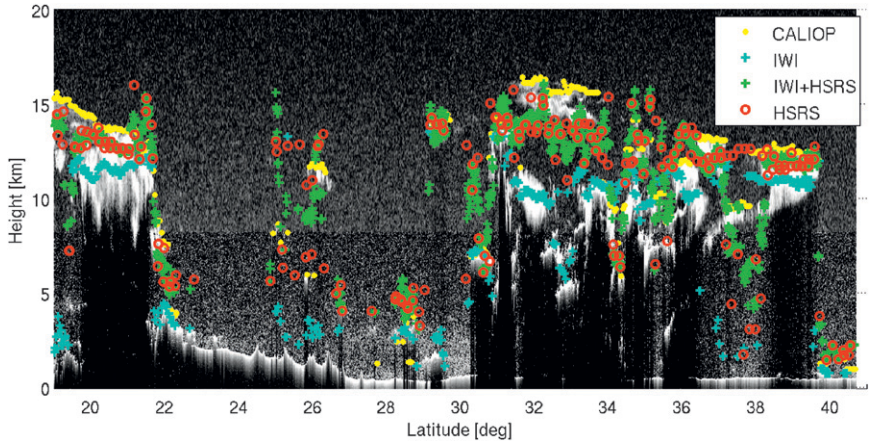

FIG. 8. As in Fig. 6, but for AIRS granule 87.

The MG method will be of particular importance with data from the JPSS satellites (e.g., Suomi NPP). Although the new VIIRS imager has many advances over previous sensors, it lacks IR bands that are sensitive to absorption by carbon dioxide or water vapor. The use of such bands provides greater sensitivity to CTP estimation than can be obtained from use of IR-window bands alone. The lack of absorbing IR bands will have the most impact on the inference of cloud-top pressure for semitransparent ice clouds. The CrIS on Suomi NPP, with sounding bands in

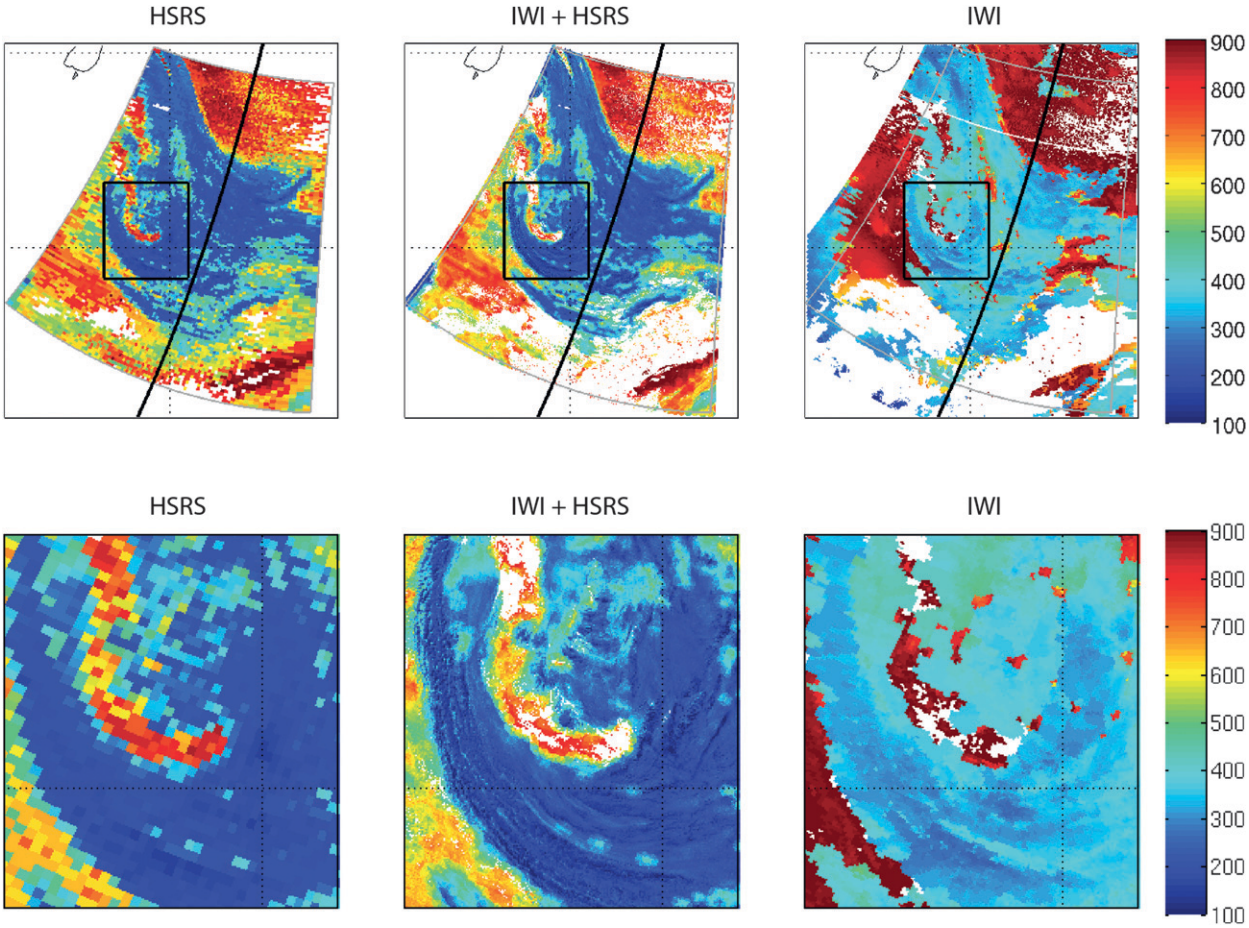

FIG. 9. As in Fig. 5, but for AIRS granule 124.

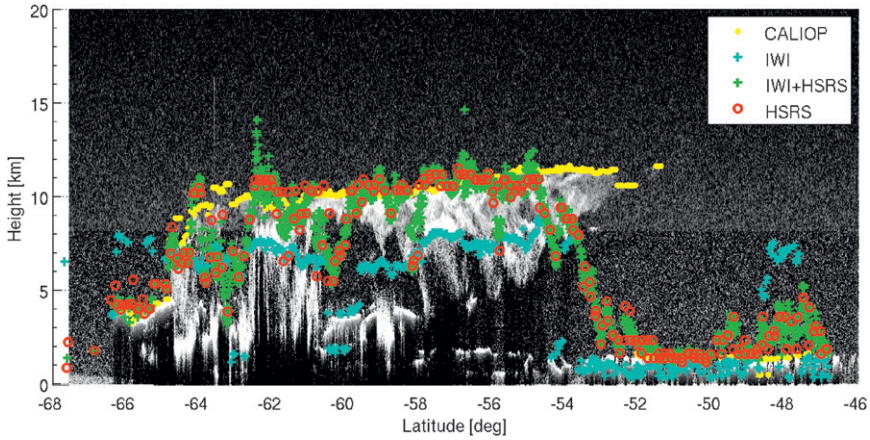

FIG. 10. As in Fig. 6, but for AIRS granule 124.

both the CO_2 and H_2O spectral regions, offers complementary measurements to VIIRS but at lower spatial resolution. CrIS is better suited to infer cloud-top pressure for cirrus because of the high-spectral-resolution sounding measurements in the CO_2 and H_2O absorption bands, whereas VIIRS is able to detect clouds of small horizontal extent and describe clouds with large horizontal variations. The same situation is found on MetOp with the AVHRR and IASI.

The MG approach is expected to make the largest contribution to IWI–HSRS instrument pairs where the IWI does not have any IR-absorbing spectral bands such as is the case with the VIIRS–CrIS and AVHRR–IASI pairs. Because the MG retrieval depends on the performance of the sounder retrieval algorithm, the improvement of the latter (e.g., by implementing a physical iterative retrieval scheme and enabling retrieval of multilayer clouds) is an important part of ongoing studies. In addition, more validation case studies of the MG IWI + HSRS algorithm could provide insight into its performance with diverse cloud conditions. Future research will also focus on investigating the sensitivity of the MG algorithm to different regression relationships. Examples include the effect of dependent versus independent coefficient sets, classifying the latter according to latitude, applying a distance-weighting function to IWI pixels in the retrieval FOI, and reducing the coefficient neighborhood definition to 3×3 HSRS FOVs instead of 5×5, as it is currently. We ultimately envisage that the MG algorithm will improve the estimation of cirrus-cloud distributions regionally and globally.

Acknowledgments. This project was supported by NASA Grants NNX08AG96G and NNX11AK22G. The authors acknowledge with gratitude the Goddard Earth Sciences Data and Information Services Center (GES DISC) for AIRS L1B data, the L1B Atmospheric Archive and Distribution System (LAADS) for MODIS data, the CloudSat Data Processing Center for *CloudSat* data, and the NASA Langley Atmospheric Science Data Center (ASDC) for *CALIPSO* data; Dr. Andrew Heidinger provided the VIIRS processing of the selected granules. The authors also express their appreciation to Dr. Robert Holz for many useful discussions and to the three reviewers who helped us to substantially improve the manuscript.

REFERENCES

Ackerman, S. A., K. I. Strabala, W. P. Menzel, R. A. Frey, C. C. Moeller, and L. E. Gumley, 1998: Discriminating clear sky from clouds with MODIS. *J. Geophys. Res.,* **103,** 32 141–32 157.

——, R. E. Holz, R. Frey, E. W. Eloranta, B. C. Maddux, and M. McGill, 2008: Cloud detection with MODIS. Part II: Validation. *J. Atmos. Oceanic Technol.,* **25,** 1073–1086.

Aumann, H. H., and Coauthors, 2003: AIRS/AMSU/HSB on the *Aqua* mission: Design, science objective, data products, and processing systems. *IEEE Trans. Geosci. Remote Sens.,* **41,** 253–264.

Barnes, W. L., T. S. Pagano, and V. V. Salomonson, 1998: Prelaunch characteristics of the Moderate Resolution Imaging Spectroradiometer (MODIS) on EOS-AM1. *IEEE Trans. Geosci. Remote Sens.,* **36,** 1088–1100.

Chahine, M. T., and Coauthors, 2006: Improving weather forecasting and providing new data on greenhouse gases. *Bull. Amer. Meteor. Soc.,* **87,** 911–926.

Frey, R. A., S. A. Ackerman, Y. Liu, K. I. Strabala, H. Zhang, J. R. Key, and X. Wang, 2008: Cloud detection with MODIS. Part I: Improvements in the MODIS cloud mask for Collection 5. *J. Atmos. Oceanic Technol.,* **25,** 1057–1072.

Heidinger, A. K., and M. J. Pavolonis, 2009: Gazing at cirrus clouds for 25 years through a split window. Part I: Methodology. *J. Appl. Meteor. Climatol.,* **48,** 1100–1116.

——, ——, R. E. Holz, B. A. Baum, and S. Berthier, 2010: Using *CALIPSO* to explore the sensitivity to cirrus height in the infrared observations from NPOESS/VIIRS and GOES-R/ABI. *J. Geophys. Res.,* **115,** D00H20, doi:10.1029/2009JD012152.

Holz, R. E., S. A. Ackerman, F. W. Nagle, R. Frey, S. Dutcher, R. E. Kuehn, M. Vaughan, and B. A. Baum, 2008: Global MODIS

cloud detection and height evaluation using CALIOP. *J. Geophys. Res.,* **113,** D00A19, doi:10.1029/2008JD009837.

Kahn, B. H., E. Fishbein, S. L. Nasiri, A. Eldering, E. J. Fetzer, M. J. Garay, and S.-Y. Lee, 2007: The radiative consistency of Atmospheric Infrared Sounder and Moderate Resolution Imaging Spectroradiometer cloud retrievals. *J. Geophys. Res.,* **112,** D09201, doi:10.1029/2006JD007486.

——, ——, ——, ——, ——, M. J. Garay, and S.-Y. Lee, 2008: Cloud type comparisons of AIRS, *CloudSat*, and *CALIPSO* cloud height and amount. *Atmos. Chem. Phys.,* **8,** 1231–1248.

King, M. D., Y. J. Kaufman, W. P. Menzel, and D. Tanre, 1992: Remote sensing of cloud, aerosol and water vapor properties from the Moderate Resolution Imaging Spectrometer (MODIS). *IEEE Trans. Geosci. Remote Sens.,* **30,** 2–27.

Li, J., W. P. Menzel, W. Zhang, F. Sun, T. J. Schmit, J. Gurka, and E. Weisz, 2004: Synergistic use of MODIS and AIRS in a variational retrieval of cloud parameters. *J. Appl. Meteor.,* **43,** 1619–1634.

——, and Coauthors, 2005: Retrieval of cloud microphysical properties from MODIS and AIRS. *J. Appl. Meteor.,* **44,** 1526–1543.

Mace, G. G., R. Marchand, Q. Zhang, and G. Stephens, 2007: Global hydrometeor occurrence as observed by *CloudSat*: Initial observations from summer 2006. *Geophys. Res. Lett.,* **34,** L09808, doi:10.1029/2006GL029017.

Marchand, R., G. G. Mace, T. Ackerman, and G. Stephens, 2008: Hydrometeor detection using *CloudSat*—An Earth-orbiting 94-GHz cloud radar. *J. Atmos. Oceanic Technol.,* **25,** 1057–1072.

Nagle, F. W., and R. E. Holz, 2009: Computationally efficient methods of collocating satellite, aircraft, and ground observations. *J. Atmos. Oceanic Technol.,* **26,** 1585–1595.

Smith, W. L., E. Weisz, S. Kirev, D. K. Zhou, Z. Li, and E. E. Borbas, 2012: Dual-regression retrieval algorithm for real-time processing of satellite ultraspectral radiances. *J. Appl. Meteor. Climatol.,* **51,** 1455–1476.

Stephens, G. L., and Coauthors, 2002: The *CloudSat* mission and the A-Train: A new dimension of space-based observations of clouds and precipitation. *Bull. Amer. Meteor. Soc.,* **83,** 1771–1790.

Strabala, K. I., S. A. Ackerman, and W. P. Menzel, 1994: Cloud properties inferred from 8–12-μm data. *J. Appl. Meteor.,* **33,** 212–222.

Tobin, D. C., H. E. Revercomb, C. C. Moeller, and T. S. Pagano, 2006: Use of Atmospheric Infrared Sounder high-spectral resolution spectra to assess the calibration of Moderate Resolution Imaging Spectroradiometer on EOS *Aqua*. *J. Geophys. Res.,* **111,** D09S05, doi:10.1029/2005JD006095.

Wang, Z., and K. Sassen, 2001: Cloud type and macrophysical property retrieval using multiple remote sensors. *J. Appl. Meteor.,* **40,** 1665–1682.

Weisz, E., H.-L. Huang, J. Li, E. E. Borbas, and K. Baggett, 2007a: International MODIS and AIRS processing package: AIRS products and applications. *J. Appl. Remote Sens.,* **1,** 0135519, doi:10.1117/1.2766867.

——, J. Li, J. Li, D. K. Zhou, H.-L. Huang, M. D. Goldberg, and P. Yang, 2007b: Cloudy sounding and cloud-top height retrieval from AIRS alone single field-of-view radiance measurements. *Geophys. Res. Lett.,* **34,** L12802, doi:10.1029/2007GL030219.

——, ——, W. P. Menzel, A. K. Heidinger, B. H. Kahn, and C.-Y. Liu, 2007c: Comparison of AIRS, MODIS *CloudSat* and *CALIPSO* cloud top height retrievals. *Geophys. Res. Lett.,* **34,** L17811, doi:10.1029/2007GL030676.

——, W. L. Smith, J. Li, W. P. Menzel, and N. Smith, 2011: Improved profile and cloud top height retrieval by using dual regression on high-spectral resolution measurements. *Proc. Hyperspectral Imaging and Sounding of the Environment (HISE),* Toronto, ON, Canada, Optical Society of America, Paper HWA4.

Winker, D. M., M. A. Vaughan, A. Omar, Y. Hu, K. A. Powell, Z. Liu, W. W. Hunt, and S. A. Young, 2009: Overview of the *CALIPSO* mission and CALIOP data processing algorithms. *J. Atmos. Oceanic Technol.,* **26,** 2310–2323.

Wong, E., K. D. Hutchison, S. C. Ou, and K. N. Liou, 2007: Cirrus cloud top temperatures retrieved from radiances in the National Polar-Orbiting Operational Environmental Satellite System-Visible Infrared Imager Radiometer Suite 8.55 and 12.0 μm bandpasses. *Appl. Opt.,* **46,** 1316–1325.

Zhou, D. K., W. L. Smith Sr., X. Liu, A. M. Larar, S. A. Mango, and H.-L. Huang, 2007: Physically retrieving cloud and thermodynamic parameters from ultraspectral IR measurements. *J. Atmos. Sci.,* **64,** 969–982.

——, ——, A. M. Larar, X. Liu, J. P. Taylor, P. Schlüssel, L. L. Strow, and S. A. Mango, 2009: All weather IASI single field-of-view retrievals: Case study—validation with JAIVEX data. *Atmos. Chem. Phys.,* **9,** 2241–2255.